Phosphorylating Titin's Cardiac N2B Element by ERK2 or CaMKIIδ Lowers the Single Molecule and Cardiac Muscle Force

John Perkin,[1] Rebecca Slater,[1] Giorgia Del Favero,[1,2] Thomas Lanzicher,[1,2] Carlos Hidalgo,[1] Brian Anderson,[1] John E. Smith III,[1] Orfeo Sbaizero,[2] Siegfried Labeit,[3] and Henk Granzier[1,*]

[1]Department of Cellular and Molecular Medicine, University of Arizona, Tucson, Arizona; [2]Engineering and Architecture Department, University of Trieste, Trieste, Italy; and [3]Department of Integrative Pathophysiology, Medical Faculty Mannheim, University of Heidelberg, Heidelberg, Germany

ABSTRACT Titin is a large filamentous protein that is responsible for the passive force of the cardiac sarcomere. Titin's force is generated by its I-band region, which includes the cardiac-specific N2B element. The N2B element consists of three immunoglobulin domains, two small unique sequence insertions, and a large 575-residue unique sequence, the N2B-Us. Posttranslational modifications of the N2B element are thought to regulate passive force, but the underlying mechanisms are unknown. Increased passive-force levels characterize diastolic stiffening in heart-failure patients, and it is critical to understand the underlying molecular mechanisms and identify therapeutic targets. Here, we used single-molecule force spectroscopy to study the mechanical effects of the kinases calcium/calmodulin-dependent protein kinase II delta (CaMKIIδ) and extracellular signal-regulated kinase 2 (ERK2) on the single-molecule mechanics of the N2B element. Both CaMKIIδ and ERK2 were found to phosphorylate the N2B element, and single-molecule force spectroscopy revealed an increase in the persistence length (Lp) of the molecule, indicating that the bending rigidity of the molecule was increased. Experiments performed under oxidizing conditions and with a recombinant N2B element that had a simplified domain composition provided evidence that the Lp increase requires the N2B-Us of the N2B element. Mechanical experiments were also performed on skinned myocardium before and after phosphorylation. The results revealed a large (~30%) passive force reduction caused by CaMKIIδ and a much smaller (~6%) reduction caused by ERK2. These findings support the notion that the important kinases ERK2 and CaMKIIδ can alter the passive force of myocytes in the heart (although CaMKIIδ appears to be more potent) during physiological and pathophysiological states.

INTRODUCTION

During the diastolic phase of the cardiac cycle, the ventricular chamber fills, cardiac myocytes are stretched, and a resistive force is developed by the giant protein titin (1,2). Single molecules of titin span half of each sarcomere, or contractile unit of muscle, from the Z-disk to the M-band (3,4). The portion of titin that is located in the I-band region of the sarcomere contributes greatly to muscle elasticity (5–7). Due to alternative splicing, there are three different cardiac isoform classes of titin (8,9). The I-band region of all isoforms contains tandem immunoglobulin (Ig) segments (serially linked Ig domains), a PEVK element (rich in proline (P), glutamate (E), valine (V) and lysine (K)), and the N2B element (10). The N2B element is cardiac specific and consists of a large 575-residue unique sequence (the N2B-Us), three flanking Ig domains (I24–I26), and two other smaller unique sequences (21 and 67 residues in size, respectively) (10). Importantly, the N2B-Us appears to be a hotspot for posttranslational modifications, and phosphorylation is thought to alter its mechanical state (11,12). Furthermore, deranged phosphorylation of cardiac titin characterizes heart failure with preserved ejection fraction (13–16). This type of heart failure is highly prevalent, but its molecular basis is not understood (17). Hence, it is important to understand in detail all of the changes that titin phosphorylation causes in titin's spring region.

Protein kinase A (PKA), which is activated by the β-adrenergic pathway, phosphorylates the large unique sequence of the N2B element that reduces passive muscle stiffness (18,19). Similarly to PKA, protein kinase G (PKG), a cGMP-dependent kinase that is part of signaling cascades initiated by nitric oxide and natriuretic peptides, phosphorylates the unique sequence of the N2B element and reduces passive stiffness. The PKG phosphorylation site in humans is S4185 (the numbering system used in this work is based on the canonical human titin sequence UniProtKB Q8WZ42-1), which is also a residue phosphorylated by PKA (20,21). More recently, it was discovered that the N2B element of cardiac titin is a target of calcium/calmodulin-dependent protein kinase II delta (CaMKIIδ) (21,22). CaMKIIδ is the predominant CaMKII isoform in the heart (23), where it phosphorylates several

Accepted for publication November 4, 2015.

*Correspondence: granzier@email.arizona.edu

Giorgia Del Favero's present address is Department of Food Chemistry and Toxicology, University of Vienna, Vienna, Austria.

John Perkin and Rebecca Slater contributed equally to this work.

Ca^{2+}-handling proteins, including phospholamban (PLB) (24), ryanodine receptor (RyR2) (25), and L-type Ca^{2+} channel (LTCC) (26), as well as the myofilament proteins TnT (27) and MyBP-C (28). We previously showed that phosphorylation of titin by CaMKIIδ occurs in vivo, including during ischemia/reperfusion (IR) injury, which is known to activate CaMKIIδ (29). IR injury induces an increase in the phosphorylation level of CaMKIIδ sites on titin, and this is abolished by the CaMKIIδ inhibitor KN-93 (22). There are nine serine and threonine residues in the N2B-Us that are phosphorylated by CaMKIIδ (21,22). Two of these sites (S3750 and S4209) are highly conserved among mammals, suggesting their importance in the regulation of titin's elastic properties (11,12). Another kinase that was recently shown to target sites located in the N2B-Us of titin is extracellular signal-regulated kinase 2 (ERK2) (30). ERK2 phosphorylates three serines in titin's N2B-Us: S3918, S3960, and S4010 (the latter of which is well conserved) (11,30). It has been proposed that ERK2-based phosphorylation lowers titin-based passive tension (30), but experimental evidence for this proposal is lacking. In this work, we used single-molecule force spectroscopy (31) to examine the effect of CaMKIIδ and ERK2 phosphorylation on single-molecule mechanics, which has not been studied before. We also examined muscle mechanics (32) and studied the effects of CaMKIIδ and ERK2 on passive stress using a repeated stretch-release protocol that mimics the heart cycle.

MATERIALS AND METHODS

Protein constructs

Two different recombinant protein constructs were used in this study. The first consisted of the entire human titin exon 49 sequence (I24–I26), N2B-Us, and intermediate unique sequences (Fig. 1 *A*). The sequence was amplified by PCR from total human cDNAs, and primer pairs were derived from the human cardiac titin N2B isoform. The pETM-11 constructs were transformed into BL21(DE3) pLysS cells, and isopropyl β-D-1-thiogalactopyranoside (IPTG)-induced proteins were purified from the soluble fraction on Ni^{2+}-nitrilotriacetic acid (NiNTA) columns (taking advantage of the N-terminal 6XHis tag provided by the vector), quick-frozen, and stored at −80°C until later use. The second construct was a modified version and contained only the N2B-Us flanked by two I24 domains on either side, with no unique sequences in between (see Fig. 5 *A*). The expression construct (synthesized by DNA2.0) had the IPTG-inducible pJexpress vector backbone and included an N-terminal 6XHis-tag and two cysteine residues at the C-terminus to aid in attachment to gold-coated substrates. The induced protein was purified on NiNTA columns, quick-frozen, and stored at −80°C until later use. The purified proteins were then either phosphorylated with ERK2 or CaMKIIδ, or left unphosphorylated to serve as controls. To determine the optimum phosphorylation level of the N2B-Us, various concentrations of CaMKIIδ were used, followed by analysis using a 10% SDS-PAGE and a Pro Q-Diamond phospho-stain. The gel was then stained with Coomassie blue (CB) to determine the total protein content. The CB stain was used to normalize the Pro-Q diamond signal.

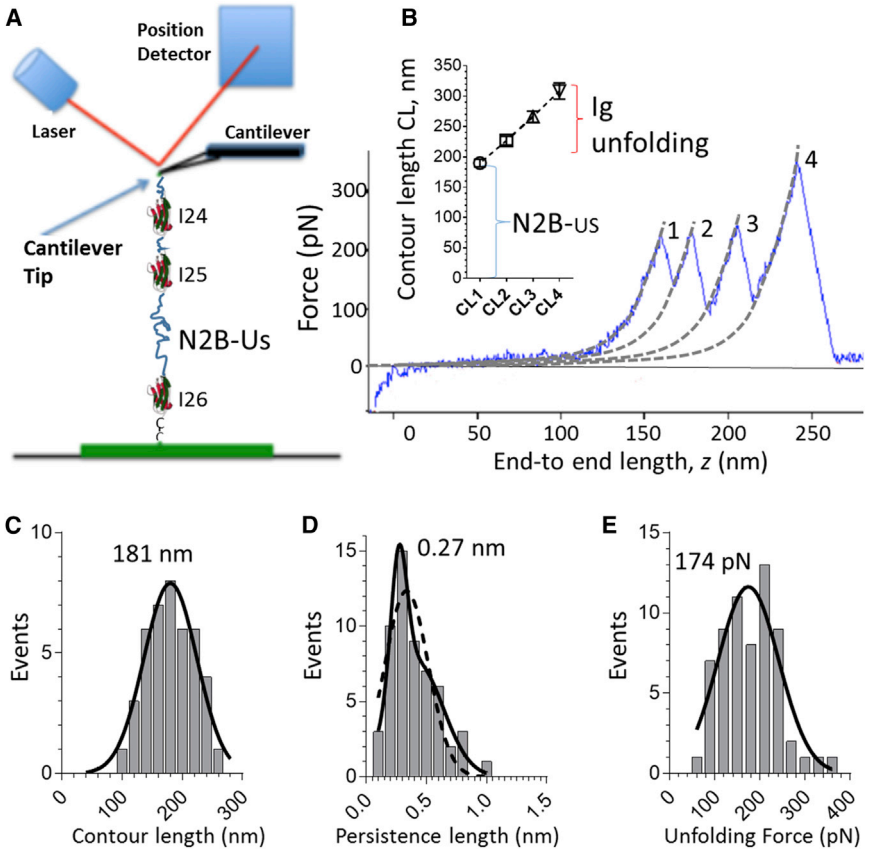

FIGURE 1 Single-molecule mechanics on titin's N2B element. (*A*) Schematic of an N2B molecule tethered between a microscope slide and cantilever tip. (*B*) Example of a force-extension curve of the N2B molecule. Three force peaks are present due to Ig domain unfolding, and a fourth peak represents the molecule breaking loose from the cantilever. Force curves were fit by the WLC equation; contour length (Lc) values are shown in the inset. The Lc of the first peak is due to the N2B-Us, and the subsequent Lc values indicate gains due to Ig domain unfolding. (*C*) Lc histogram of N2B-US. (*D*) Persistence length (Lp) histogram of N2B-Us. (*E*) Unfolding force (Uf) of Ig domains. Results were fit by Gaussian curves; peaks are shown on the graph. To see this figure in color, go online.

The obtained dose-response curve (Fig. 2) indicated that a CaMKIIδ concentration of 0.075 U/μL maximally phosphorylated the N2B recombinant protein. For ERK2 phosphorylation, the level was determined to be 1.5 U/μL (Fig. 2 *B*). Aliquots of the protein were frozen at −80°C. For each experiment, one aliquot of protein was thawed and incubated on a glass slide in a buffer solution (25 mM BES, 2.5 mM EGTA, 1.5 mM $MgCl_2$, 1.25 mM NaATP, 165 mM KCl, 5 mM dithiothreitol (DTT; omitted for the experiments under oxidizing conditions), pH 7.0). The concentration of recombinant protein in buffer solution was ~0.5 nM. The reducing agent DTT (1 mM) was added fresh to prevent the formation of disulfide bridges within the N2B unique sequence, but in other experiments DTT was omitted so that the effect of disulfide cross-links on the mechanical properties of the N2B molecule could be studied (33).

Single-molecule force spectroscopy

An MFP3D atomic force microscope (Asylum Research, Santa Barbara, CA) was used for force spectroscopy. To determine the spring constant of the cantilever (model MLCT; Bruker), a thermal calibration was conducted (typical values were 15–25 pN/nm). After the calibration, the cantilever tip was used to probe the surface of the gold-coated glass slide. The piezo motor moved the cantilever up and down, and was set to operate at a pulling velocity of 1000 nm/s. The cantilever tip approached and retracted from the surface of the slide, and when an extension/retraction force curve was obtained, it was evaluated as to whether it displayed a low-force region (extension of the N2B-Us) followed by several regularly spaced (~30 nm) sawtooth force peaks (one for each Ig domain present) and one final larger-force detachment peak (Fig. 1 *B*). Curves were analyzed using the wormlike-chain (WLC) equation (34,35):

$$F = \frac{k_B T}{L_p}\left(\frac{1}{4\left(1-\frac{z}{L_c}\right)^2}-\frac{1}{4}+\frac{z}{L_c}\right),$$

where F is the force, k_BT is the thermal energy (k_B is Boltzmann's constant and T is the absolute temperature), Lp is the persistence length of the molecule, Lc is the contour length, and z is the end-to-end length of the molecule. The Lp is the minimal distance along the backbone of the molecule over which tangent lines are correlated, or, in other words, Lp describes the inverse of the propensity of the molecule to collapse. An increase in Lp after phosphorylation effectively means that the molecule extends more for the same force. At the cardiac myocyte level, this corresponds to a more compliant myocardium. Most curves had a smooth initial low force-extension phase, but some had small force peaks at several tens of piconewtons. The results of these curves were grouped with those for the rest of the molecules in which such small force bumps were absent.

Skinned muscle mechanics

Papillary muscles were harvested from 3-month-old female mice on a C57BL/6 background. All experiments were performed in accordance with the NIH Guide for the Care and Use of Laboratory Animals and approved by the IACUC of the University of Arizona. Muscle preparations were dissected as previously described (36). The skinned muscle was treated with 0.5 U/μL protein phosphatase 1 (recombinant rabbit muscle α-isoform; Calbiochem) for 2 h and then washed extensively in relaxing solution. Fiber bundles were secured to a servo-motor (308B; Aurora) and force transducer (AE801; SensorOne) on either end with aluminum T-clips in a bath of relaxing solution. Tension and sarcomere length (SL) were recorded simultaneously with the force transducer and a laser diffraction system with a spatial resolution of ~10 nm/sarcomere and a time solution of 2 ms. Muscle bundles were set to slack SL (defined as SL with zero passive stress). We determined the slack SL by shortening the passive muscle until it clearly buckled, holding it there for 10 min, and then stretching the muscle to the minimum length at which the buckle was taken up and no detectable passive force developed, at which point we measured the SL by laser diffraction (~1.85–1.9 μm). We used the active tension as a measure of tissue health by activating the skinned fibers with pCa 4.0 activating solution (36) (typical values were 30–40 mN/mm^2). After the slack length was determined and the tissue was activated and relaxed, it underwent a series of tandem triangle stretches from slack to an SL of 2.2 μm at 300%/s for 1000 cycles. (The stretch speed and maximal SL approximate the physiological conditions during diastole (37).) The solution in the bath was then replaced with relaxing solution containing kinases with and without kinase inhibitors (for the control experiment). In the CaMKIIδ study, preactivated CaMKIIδ (0.26 U/μL, recombinant human; Life Technologies) was added in the absence or presence of 0.06 mM Autocamtide-2-Related Inhibitory Peptide II (AIP-II; Calbiochem). Similarly, for the Erk2 study, the solution contained 31.2 U/μL Erk2 (recombinant human; Calbiochem) in the absence or presence of 0.14 μM Erk Inhibitor II (FR180204; Calbiochem). The fiber bundle was incubated at room temperature in the kinase/inhibitor solution for 3 h (to ensure optimal phosphorylation), with a stretch to an SL of 2.1 μm every 5 min. Finally, the bundle was thoroughly washed with relaxing solution before the same series of stretch/release cycles described above was repeated.

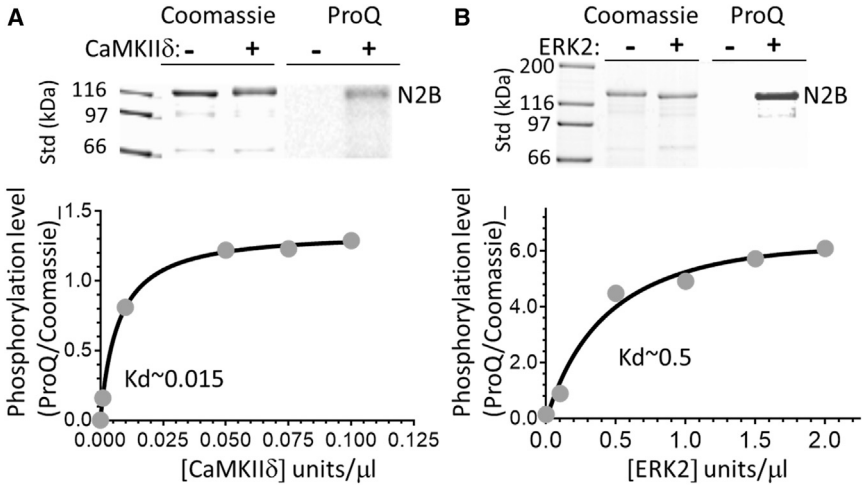

FIGURE 2 (*A* and *B*) The N2B element is a CaMKIIδ (*A*) and ERK2 substrate (*B*). Top: in vitro kinase assays with the protein gel stained by Coomassie blue (*left*) and the corresponding ProQ Diamond phospho-stained image (*right*). Bottom: phosphorylation level (ProQ/Coomassie) versus kinase concentration.

WLC simulations

The force-SL relation of a single titin molecule (N2B cardiac titin isoform) was calculated using the WLC equation (38), with three serially linked WLCs representing the combined proximal and distal tandem Ig segments, the PEVK, and N2B-Us spring elements (39). The Lc of the tandem Ig segments was 200 nm (40 Ig domains with an average spacing of 5 nm). The PEVK Lc was 70 nm and the N2B-Us Lc was 180 nm. The Lp values were 12 nm (tandem Ig segments), 1.0 nm (PEVK), 0.3 nm (dephosphorylated N2B-Us), and 0.6 (phosphorylated N2B-Us). (For experimental evidence that underlies these values and additional details, see previous studies (39–42) and Results. Note that for simplicity's sake, the simulation does not take into account the bimodal Lp distribution that was found.) The force-SL relation of a single titin molecule was then calculated and the results were compared for phosphorylated molecules and molecules with dephosphorylated N2B-Us (see Fig. 7 *A*). At an SL of 2.2 μm (selected because at this length the fractional extension of the N2B element is >0.1, which avoids volume-exclusion and self-interaction effects (34,35), and this SL is near the upper limit of the physiological SL range), the force difference due to N2B-Us phosphorylation was calculated and compared with the tissue-mechanics results.

Statistical analysis

The effects of phosphorylation on the Lp, Lc, and unfolding force (Uf) were analyzed using a two-tailed *t*-test, and $p < 0.05$ was taken as significant. (The same results were obtained when a nonparametric Mann-Whitney test was used.) Values were also plotted in histograms that were fit with Gaussian curves (GraphPad Prism). For the skinned-muscle data, mean and SEM force values were calculated at each cycle number (see Fig. 6) and results were fit with a two-phase-decay equation. A statistical analysis was performed (GraphPad Prism) to test whether the two data sets (results after kinase treatment and after kinase + inhibitor treatment) were best fit by one or two equations (see Fig. 6). A nonlinear regression was performed with an extra sum-of-squares F test to determine whether there was evidence that the data sets differed from each other. The simpler model (i.e., single equation) was preferred for *p*-values > 0.05.

RESULTS

Single-molecule force spectroscopy

Titin's N2B element is a cardiac-specific spring that functions as a phosphorylation hotspot, and we investigated the effects of CaMKIIδ and ERK2 using single-molecule force spectroscopy and tissue mechanics. Fig. 1 *A* shows a schematic of an N2B molecule tethered between a microscope slide and cantilever tip. The native N2B element consists of a large unique sequence (N2B-Us, 575 residues) flanked at one end by I26 and at the other by I24 and I25 (separated by a short 21-residue unique sequence) and a terminal 67-residue unique sequence. An example of a force-extension curve is depicted in Fig. 1 *B*. There is an initial low-force phase (due to extension of the N2B-Us) followed by three force peaks (due to Ig domain unfolding), and a fourth peak representing the molecule breaking loose from the cantilever. Force curves were fit by using the WLC equation (*broken lines* in Fig. 1 *B*) and the Lc and Lp were determined. The mean Lc data are shown in the inset of Fig. 1 *B*. The Lc of the first peak (~180 nm) and the subsequent Lc gain (~35 nm) are likely due to the N2B-Us and Ig domain unfolding, respectively. The Lc histogram of the N2B-Us is fairly broad (Fig. 1 *C*) and can be fitted with a single Gaussian with a maximum at 181 nm. The Lp distribution of the N2B-Us ranges from ~0.2 to ~0.8 nm and can be fit with a single Gaussian curve (*broken curve* in Fig. 1 *D*) or, with a slightly better r^2, by the sum of two Gaussians, with a main peak at 0.27 nm (*solid curve* in Fig. 1 *D*). The Ig domain Uf histogram (all values were grouped) ranged from ~100 to 300 pN, with a Gaussian curve fit that had a maximum at 174 pN (Fig. 1 *E*). Thus, force spectroscopy on the N2B molecule makes it possible to characterize the properties of the N2B-Us and examine how it is affected by phosphorylation.

Effect of CaMKIIδ and ERK2 on N2B-Us

In vitro kinase assays showed that the N2B element is a good substrate for both kinases (Fig. 2), confirming earlier findings (21,22,30).

Force spectroscopy on phosphorylated molecules did not reveal any easily detectable change, but when N2B-Us Lp values were plotted in a histogram, a shift to larger values became apparent in both CaMKIIδ- and ERK2-treated samples (Fig. 3). ERK2 data were fit best by the sum of two Gaussians with peaks at 0.36 and 0.67 nm, and CaMKIIδ data were fit best by a single Gaussian phosphorylated with a peak at 0.48 nm. The bimodal distribution of the ERK2 data set might reflect incomplete phosphorylation or the presence of more than one phosphorylation site. A comparison of the unphosphorylated and phosphorylated data sets revealed a significantly increased Lp in ERK2 and CaMKIIδ. No differences were observed for Uf values (Table 1). We noted a reduction in Lc values after phosphorylation, which possibly reflects the formation of phosphorylation-induced stable structures, but the Lc reduction was not statistically significant and thus might also be a random effect.

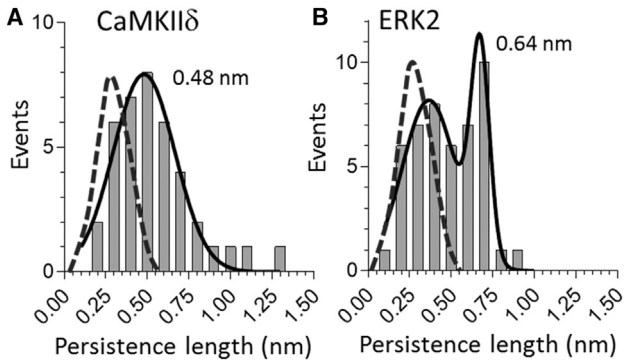

FIGURE 3 (*A* and *B*) Effect of CaMKIIδ (*A*) and ERK2 (*B*) on the Lp of N2B-Us. After phosphorylation, the Lp distribution is shifted to the right from that of unphosphorylated molecules (indicated by *broken curves*; same data as in Fig. 1). The values shown are peak positions of Gaussian fits.

TABLE 1 Effect of CaMKIIδ and ERK2 on Single N2B Molecule Characteristics

I24–I26 N2B	Control	CamKIIδ	ERK2
Lp, nm	0.37 ± 0.02 ($n = 53$)	0.47 ± 0.02* ($n = 53$)	0.47 ± 0.03* ($n = 50$)
Lc, nm	189 ± 7 ($n = 53$)	171 ± 10 ($n = 53$)	172 ± 7 ($n = 50$)
Uf, pN	173 ± 9 ($n = 112$)	174 ± 9 ($n = 96$)	163 ± 6 ($n = 107$)
(I24)x4 N2B	**Control**	**CaMKIIδ**	
Lp, nm	0.25 ± 0.03 ($n = 36$)	0.47 ± 0.06** ($n = 33$)	
Lc, nm	195 ± 7 ($n = 53$)	180 ± 6 ($n = 33$)	
Uf, pN	173 ± 5 ($n = 114$)	152 ± 7* ($n = 109$)	

Lp, persistence length; Lc, contour length; Uf, unfolding force.
*$p < 0.05$.
**$p < 0.01$.

Considering that the native N2B molecule also has small unique sequences flanking I24 (21 and 67 residues, respectively) that potentially contain phosphorylation sites, we sought to determine for both ERK2 and CaMKIIδ whether the phosphorylation effect was indeed due to the large unique N2B-Us sequence. For ERK2, we followed up on work by Leake et al. (33), who performed experiments under oxidizing conditions and showed that the N2B-Us forms disulfide cross-links. The N2B-Us contains six cysteines, and all possible cross-link combinations and how they reduce Lc are shown in Fig. 4 *A*. (Cysteines are absent from the short unique sequences that flank I24.) The notion that cross-linking occurs in the N2B-Us is supported by a previous study in which oxidizing conditions resulted in an increase in passive stiffness in skinned muscle from wild-type mice, but not in mice from which the N2B-Us had been deleted (32). In this study, we found that the measured Lc histogram of the N2B-Us under oxidizing conditions was distinct from that obtained in the presence of DTT. The distribution was bimodal with a major peak at 107 nm and a minor peak at 195 nm (Fig. 4 *B*). Since the latter peak overlaps that of the Lc measured with DTT (reproduced in Fig. 4 *B* by the *broken curve*), it is likely that this reflects the uncross-linked N2B-Us and the peak at the shorter-length cross-linked N2B-Us. Thus, cross-linking shortened the Lc of a large fraction of the molecules by ~90 nm. This value is consistent with cross-links between cysteines 1 and 3, and cysteines 2 and 4 (Fig. 4 *A*, *right*). Since this hides ERK phospho-sites (two of the three sites for one to three cross-links, and all three sites for two to four cross-links), the effect of ERK2 phosphorylation under oxidizing conditions was studied. No ERK2 effect was found (compare Fig. 4, *C* and *D*). This supports the notion that the ERK2 effect on Lp measured under reducing conditions is due to phosphorylating N2B-Us.

To test whether the CaMKIIδ effect was based on phosphorylation of only the N2B-Us or involved any of the other unique sequences (flanking I24), we studied a construct that consisted of the N2B-Us with two flanking I24 domains ((I24)x4-N2B-Us; Fig. 5 *A*) on either side. (Note that

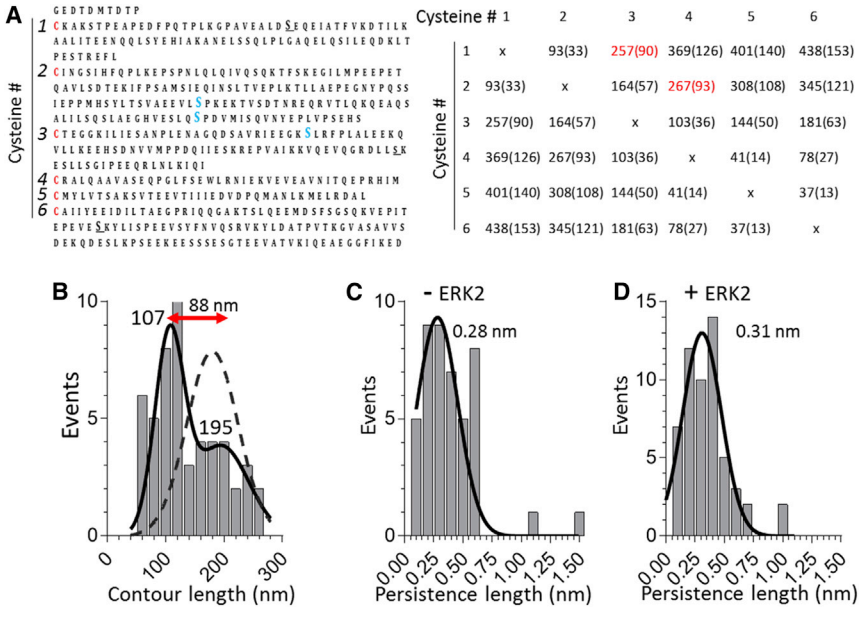

FIGURE 4 Effect of ERK2 on N2B-Us measured under oxidizing conditions. (*A*) Left: N2B-Us with its six cysteines (*red font*) and the three ERK2 phospho-sites (*blue font*). Right: all possible cross-link combinations between the six cysteines, showing the number of residues in between the cross-links and the effect of cross-linking on the Lc of the N2B-Us (shown in parentheses and calculated assuming that each reduces the Lc by 0.35 nm). (*B–D*) Measurements obtained under oxidizing conditions (no DTT). (*B*) Lc of N2B-Us. The Lc distribution can be fit with a double Gaussian with peaks at 107 and 195 nm. Broken curve: measurements under reducing conditions (from Fig. 1 *B*). The difference in peak positions (88 nm) can be explained by cross-linking between either the first and third or the second and fourth cysteines (indicated in *red* in (*A*), *right*). (*C* and *D*) ERK2 has no effect on the Lp. To see this figure in color, go online.

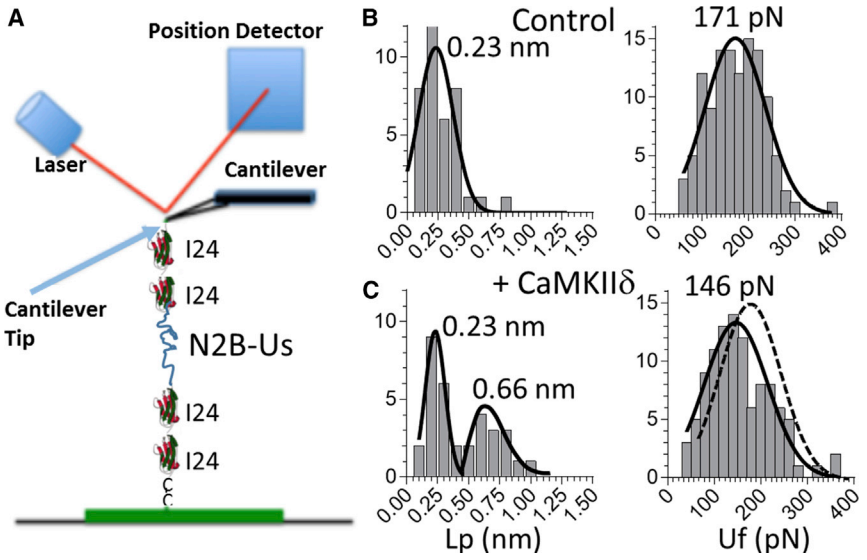

FIGURE 5 Effect of CaMKIIδ on the single-molecule mechanics of (I24)x4-N2B-Us molecules. (*A*) The N2B molecule consists of a large unique sequence (N2B-Us) flanked at both ends by two identical I24 domains. (*B* and *C*) Lp (*left*) and Uf (*right*) distribution of unphosphorylated molecules (*top*: control; *bottom*: CaMKIIδ phosphorylated). To see this figure in color, go online.

studying molecules that have disulfide cross-links is not a good option for CaMKIIδ because there are many phospho-sites (12), including outside the cysteine-containing region of the N2B-Us.) The N2B-Us Lp and Uf of the unphosphorylated (I24)x4-N2B-Us molecules were indistinguishable from those of the native N2B molecule (Fig. 5 *B* and Table 1, *bottom*). After CaMKIIδ phosphorylation, the Lp distribution was bimodal, with a new peak at 0.66 nm (Fig. 5 *C*, *left*), and when analyzed by *t*-test, Lp was found to be increased relative to unphosphorylated molecules (Table 1, *bottom*). The N2B-Us Lc was unchanged, but, interestingly, the average Uf was slightly but significantly reduced (Fig. 5 *C*, *right*). It is possible that coupling between the N2B-Us and I24 somehow caused the reduction in Uf. Alternatively, it is possible that I24 became phosphorylated and this reduced the Uf. The fact that this effect was not seen in the I24-I26-N2B-Us construct suggests that I25 and I26 were unchanged and dominated the histogram of all unfolding events. In summary, the studies on the (I24)x4-N2B-Us construct show that the effect of CaMKIIδ phosphorylation on the N2B element does not rely on the small unique sequences that flank the native I24.

Effect of CaMKIIδ and ERK2 on the passive force of skinned cardiac muscle

To determine whether our single-molecule findings have relevance for muscle, we performed mechanical experiments on passive skinned myocardium. We used a cyclic stretch/release protocol that mimics loading conditions in the heart (see Materials and Methods). For each cycle, passive stress (force per unit area) was measured at the peak of the stretch (SL 2.2 μm). All muscles were studied before and after they were incubated with kinase. In control experiments, muscles were treated the same except that in addition to kinase, a kinase inhibitor was added (see Materials and Methods), yielding two data sets (kinase and kinase + inhibitor). There was significantly less passive stress in muscles that were treated with kinase (compared with kinase + inhibitor), supporting the notion that passive stress is reduced by phosphorylation (Fig. 6, *A–C*). However, the percent stress reduction was much larger for CaMKIIδ than for ERK2 (Fig. 6 *D*). To ensure that the ERK2 treatment resulted in titin phosphorylation (it is known that CaMKIIδ phosphorylates titin in skinned muscle (21,22)), we performed ERK2 phosphorylation assays on skinned muscle. These assays showed robust phosphorylation of titin (Fig. 6, *top right*).

To gain insights into whether the large CaMKIIδ passive stress reduction (~30%) or the small ERK2 reduction (~6%) was in line with the single-molecule studies, we performed simulation experiments. Titin's spring region consists of three serially linked spring elements, and we calculated the predicted force-SL relation of a single titin molecule using a serially linked WLC model with an Lp of 0.3 for unphosphorylated N2B-Us and 0.6 nm for phosphorylated molecules (other Lc and Lp values and additional details are given in Materials and Methods). (Note that for simplicity, the multimodal distribution of Lp values was not incorporated into the simulation.) The results indicate that the predicted force was reduced in the phosphorylated state (Fig. 7), e.g., at SL 2.2 μm, the predicted force reduction was 25%.

DISCUSSION

Posttranslational modifications of titin's spring region are important for tuning passive myocardial stiffness and are likely to play an important role in the diastolic dysfunction that characterizes heart-failure patients. Here, we studied titin's N2B element, a cardiac-specific spring that functions as a phosphorylation hotspot, and investigated the effects

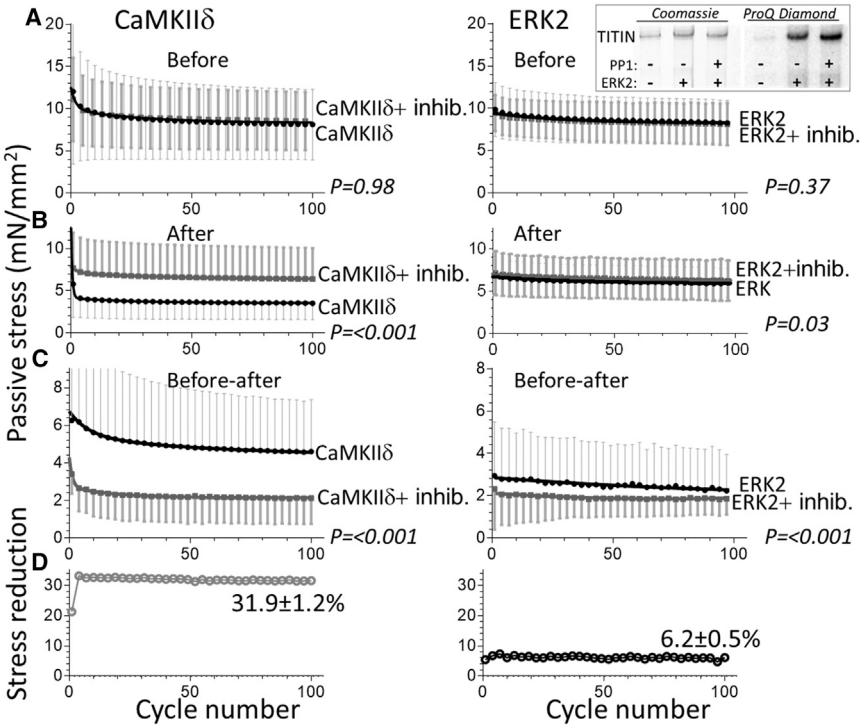

FIGURE 6 Effect of CaMKIIδ (*left*) and ERK2 (*right*) on the passive stress of skinned myocardium. Passive muscle was stretched in a cyclic manner from slack SL to an SL of 2.2 μm, followed by a release back to slack, and the peak stress was plotted versus the cycle number. (*A–C*) Results before (*A*) and after (*B*) incubation in kinase or kinase + inhibitor, and (*C*) the magnitude of stress reduction. Right: the top inset shows the effect of ERK2 on titin phosphorylation. (*D*) Left: percent reduction due to CaMKIIδ phosphorylation ((before − after)/before × 100%, corrected for a reduction in CaMKIIδ + inhibitor). Right: the same as at left, but for ERK2. The percent reduction is much larger for CaMKIIδ than for ERK2. See Materials and Methods for additional details.

of CaMKIIδ and ERK2 using single-molecule force spectroscopy and tissue mechanics. We found that both kinases increased the Lp of the N2B element and that this effect required the large unique sequence, the N2B-Us. Tissue mechanics revealed that in line with the measured Lp change, passive myocardial stress was reduced, but the effect was much larger for CaMKIIδ than for ERK2. Below, we discuss these findings and their functional implications.

The Lp distribution of the N2B-Us shifted to larger values after phosphorylation by CaMKIIδ or ERK2 and the histograms showed subpeaks, likely due to a subpopulation of unphosphorylated molecules combined with those that had been phosphorylated. The various Lp histograms that were obtained suggest that phosphorylation increased the Lp from ~0.3 to ~0.6 nm. These values can be compared with those obtained by Kruger al. (20), who studied the effect of PKG, which targets S4185 near the C-terminus of the N2B-Us, a residue that is also phosphorylated by PKA. In line with our findings, PKG phosphorylation was shown to increase the Lp from 0.31 to 0.67 nm (20). It is currently unknown how phosphorylation increases the Lp. It is possible that changes in the bending rigidity of the N2B-Us are due to the addition of negative charges and/or the existence of local structures that undergo structural transitions when phosphorylated. This important issue needs to be experimentally addressed in future work using structural techniques such as circular dichroism and Förster resonance energy transfer. In summary, together with earlier findings, our results suggest that phosphorylating the N2B-Us sequence increases Lp irrespective of the phosphorylation sites involved.

An increase in Lp at the single-molecule level is predicted to lower the passive force of the cardiac myocyte (Lp and force are inversely related), and we tested this prediction in mechanical studies on mouse papillary muscle. In these studies, we used a repeated stretch-release protocol that mimicked the physiological strain rate in the heart. We noted that passive force revealed a time-dependent

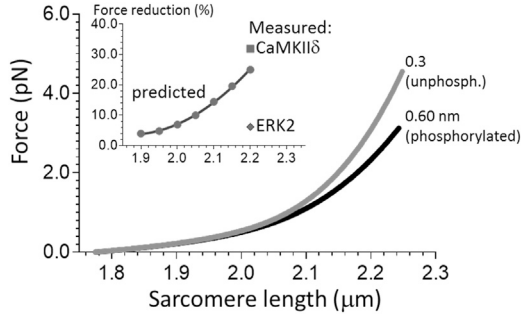

FIGURE 7 Measured and predicted effects of increasing the Lp of N2B-Us on passive force. The predicted force-SL relation of a single titin molecule was calculated using a serially linked WLC model with an N2B-Us Lp of 0.3 nm (unphosphorylated state) or 0.6 nm (phosphorylated state). (For other parameters and additional details, see Materials and Methods.) The predicted force is reduced in the phosphorylated state. The percent force reduction is shown as a function of SL in the inset. The measured force reduction at SL 2.2 μm after CaMKIIδ and ERK2 phosphorylation (data from Fig. 6 *D*) is also shown. The magnitude of the measured force reduction after CaMKIIδ phosphorylation is similar to the predicted value, but the measured ERK2 phosphorylation is considerably less than predicted.

exponential decline. These protocols started with a well-rested skinned muscle held at its slack length. We propose that in that state, nonspecific interactions form (e.g., electrostatic interactions between oppositely charged protein domains), either within subdomains of titin or between titin and other filaments. Such bonds will impede titin stretch, and thus during a repeated stretch-release protocol, the passive force will initially be high. However, the bonds are expected to break during stretch (progressively more of them as the number of stretch/release cycles increases), and consequently the force will progressively decline (only during a prolonged rest at the slack length will the bonds reform). We obtained evidence for such a mechanism in single-molecule experiments in which titin was repeatedly stretched (43). We determined the predicted effect by using a serially linked WLC model in which the three spring elements within titin's extensible region (tandem Ig segments, the PEVK, and the N2B-Us) were linked and the Lp of the N2B-Us was varied from 0.3 nm (unphosphorylated) to 0.6 nm (phosphorylated). The obtained force reductions increased with SL (the N2B-Us becomes progressively more important to titin's elasticity as the sarcomeres are stretched (41,44)), e.g., at an SL of 2.0 μm the predicted force reduction was 7%, whereas at 2.2 μm it was 25%. Phosphorylating skinned muscle with ERK2 resulted in only a small passive force reduction, ~6%, which is much less than predicted. Although titin was robustly phosphorylated when skinned muscle was exposed to ERK2 (Fig. 6, *top right*), we cannot firmly exclude the possibility that some ERK2 phosphorylation sites are not accessible due to the recently reported interaction between four-and-a-half lim (FHL) protein and the N2B-Us that inhibits ERK2 phosphorylation (30). Alternatively, since for single-molecule force spectroscopy we used an N2B construct that was based on a human sequence, but used mouse muscle to investigate tissue mechanics (human tissue was unavailable), it is also possible that the limited evolutionary conservation of the ERK2 sites (11) plays a role. Finally, it is worth noting that even modest changes in passive stiffness are likely to be functionally relevant, especially at high heart rates where filling times are short.

In contrast to the ERK2 effect, an ~30% reduction in force (SL 2.2 μm) was observed in CaMKIIδ-treated myocardium, a value that exceeds the predicted 25%. Considering the uncertainty in some of the single-molecule simulation parameters and the various sources for measurement error, both in single-molecule force spectroscopy and in muscle mechanics, the predicted and measured values (for CaMKIIδ) are quite close. It is also worth noting that CaMKIIδ phosphorylates not only the N2B-Us but also various other sites within titin (12). Of particular interest are two residues within the PEVK spring element, S11878 and S12022 (22), which when phosphorylated increase passive force (45,46). The large reduction in measured passive force clearly indicates that the N2B-Us sites dominate, which is consistent with earlier findings (22). Our muscle-mechanics results can be compared with those of Hamdani et al. (21), who measured the effect of CaMKIIδ on passive force in skinned cardiac myocytes from mice and found reductions of ~45% at an SL of 2.2 μm, which is greater than the values measured in this study. A possible explanation is that we performed control studies in the presence of CaMKIIδ and its inhibitor (which is needed because the mechanical protocol is demanding and requires long incubation times, which is likely to cause rundown, e.g., due to proteolysis or protein extraction). An interesting possibility is that the unfolding of Ig domains contributes to the force reduction, since we found that in the (I24)x4-N2B-Us construct Uf values were reduced after CaMKIIδ treatment (Fig. 5 *C*, *right*), and there is also evidence for phosphorylation by CaMKIIδ of various other I-band Ig domains (21). If Ig domain phosphorylation lowers the Uf, this could also cause a reduction in passive force that would add to the reduction that originates from the N2B element. In summary, both our studies and those of others have found robust passive force reductions after CaMKIIδ phosphorylation. The results from single-molecule force spectroscopy suggest that a large part of this reduction is readily explained by the increased Lp of titin's N2B-Us.

Physiological relevance

CaMKIIδ is the predominant CaMKII isoform in the heart, where it phosphorylates several Ca^{2+}-handling proteins (23), as well as myofilament proteins (27,28). Phosphorylation of titin by CaMKIIδ has been shown to occur in vivo under several conditions, including IR injury, a pathological state that is characterized by elevated CaMKIIδ activity and calcium overload (29,47). Recently, it was shown that IR injury induces an increase in the phosphorylation level of CaMKIIδ sites on titin, which is abolished by the CaMKIIδ inhibitor KN-93 (22). The work presented here predicts that in IR injury, CaMKIIδ-induced phosphorylation of titin will lower passive stiffness. We propose that this is a beneficial adaptation that offsets increased passive stiffness due to the known effects of calcium overload on actomyosin interaction (47). It is interesting that one of the functions of CaMKIIδ is to regulate frequency-dependent acceleration of relaxation (23,48) by phosphorylating PLB and promoting Ca^{2+} reuptake from the cytosol by SERCA, thereby maintaining efficient ventricular filling at high heart rates. Phosphorylation of the N2B element by CaMKIIδ and the ensuing decrease in titin-based passive stiffness are expected to further augment ventricular filling. Thus, it is likely that phosphorylation of titin by CaMKIIδ helps to maintain diastolic function at high heart rates. Finally, phosphorylation of histone deacetylases by CaMKII results in cardiac hypertrophy and remodeling (49), and it has been suggested that CaMKII inhibition may be a therapeutic option to treat chronic overload-induced heart disease (50).

Our work suggests that this should be done with caution, however, considering that this will abolish the beneficial effect of titin on diastolic function.

ERK2 is part of the mitogen-activated protein kinase signaling cascade (Raf1/Mek2/Erk2) with multiple downstream signaling pathways that play an important role in regulating cardiac hypertrophy and remodeling (51–53). Our work confirms the recent finding that ERK2 phosphorylates titin (30), and for the first time (to our knowledge) shows that this increases the Lp of single molecules of titin and (modestly) lowers passive stiffness in muscle. Interestingly, FHL1 and FHL2 bind the N2B-Us (30,54,55) near the ERK2 phospho-sites (30), and, importantly, binding interferes in a dose-dependent manner with ERK2-mediated N2B-Us phosphorylation (30). Thus, passive stiffness can be regulated by ERK2 activity and by regulating the availability of ERK2 phospho-sites on titin. Finally, since FHL proteins are upregulated in pressure, and volume overload induces hypertrophy (56–58), the potential for dysregulated ERK2 phosphorylation exists in these pathological states.

In conclusion, the important kinases ERK2 and CaMKIIδ regulate passive force by increasing the bending rigidity of the cardiac-specific N2B element. Although the in vivo relevance of these important findings requires further study, ERK2 and CaMKIIδ are likely to have a beneficial effect during conditions of stress when they become activated and the effects can be countered by stress-response proteins that bind to titin's N2B element.

AUTHOR CONTRIBUTIONS

Designed research: J.P., R.S., G.D.F., T.L., C.H., B.A., J.E.S., O.S., and H.G. Performed research: J.P., R.S., G.D.F., T.L., C.H., and J.E.S. Analyzed data: J.P., R.S., G.D.F., T.L., C.H., B.A., J.E.S., and H.G. Made and contributed reagents: S.L. and J.E.S. Wrote the manuscript: J.P., R.S., O.S., and H.G.

ACKNOWLEDGMENTS

We are grateful to our current and former lab members who contributed to this work.

This work was supported by National Institutes of Health grants HL062881 and HL115988, and European Union grant EU-FP7 (SarcoSi), the Foundation Leducq, and the Transatlantic Network of Excellence (14CVD03 to O.S. and T.L., and 13CVD04 to H.G. and S.L.).

REFERENCES

1. Granzier, H., Y. Wu, …, M. LeWinter. 2005. Titin: physiological function and role in cardiomyopathy and failure. *Heart Fail. Rev.* 10:211–223.
2. Wang, K., R. McCarter, …, R. Ramirez-Mitchell. 1991. Regulation of skeletal muscle stiffness and elasticity by titin isoforms: a test of the segmental extension model of resting tension. *Proc. Natl. Acad. Sci. USA.* 88:7101–7105.
3. Fürst, D. O., M. Osborn, …, K. Weber. 1988. The organization of titin filaments in the half-sarcomere revealed by monoclonal antibodies in immunoelectron microscopy: a map of ten nonrepetitive epitopes starting at the Z line extends close to the M line. *J. Cell Biol.* 106:1563–1572.
4. Wang, K. 1996. Titin/connectin and nebulin: giant protein rulers of muscle structure and function. *Adv. Biophys.* 33:123–134.
5. Granzier, H. L., and T. C. Irving. 1995. Passive tension in cardiac muscle: contribution of collagen, titin, microtubules, and intermediate filaments. *Biophys. J.* 68:1027–1044.
6. Linke, W. A., V. I. Popov, and G. H. Pollack. 1994. Passive and active tension in single cardiac myofibrils. *Biophys. J.* 67:782–792.
7. Trombitás, K., J. P. Jin, and H. Granzier. 1995. The mechanically active domain of titin in cardiac muscle. *Circ. Res.* 77:856–861.
8. Freiburg, A., K. Trombitas, …, S. Labeit. 2000. Series of exon-skipping events in the elastic spring region of titin as the structural basis for myofibrillar elastic diversity. *Circ. Res.* 86:1114–1121.
9. Cazorla, O., A. Freiburg, …, H. Granzier. 2000. Differential expression of cardiac titin isoforms and modulation of cellular stiffness. *Circ. Res.* 86:59–67.
10. Bang, M. L., T. Centner, …, S. Labeit. 2001. The complete gene sequence of titin, expression of an unusual approximately 700-kDa titin isoform, and its interaction with obscurin identify a novel Z-line to I-band linking system. *Circ. Res.* 89:1065–1072.
11. Hidalgo, C., and H. Granzier. 2013. Tuning the molecular giant titin through phosphorylation: role in health and disease. *Trends Cardiovasc. Med.* 23:165–171.
12. Linke, W. A., and N. Hamdani. 2014. Gigantic business: titin properties and function through thick and thin. *Circ. Res.* 114:1052–1068.
13. Zile, M. R., C. F. Baicu, …, M. M. LeWinter. 2015. Myocardial stiffness in patients with heart failure and a preserved ejection fraction: contributions of collagen and titin. *Circulation.* 131:1247–1259.
14. Hamdani, N., K. G. Bishu, …, W. A. Linke. 2013. Deranged myofilament phosphorylation and function in experimental heart failure with preserved ejection fraction. *Cardiovasc. Res.* 97:464–471.
15. LeWinter, M. M., and H. L. Granzier. 2014. Cardiac titin and heart disease. *J. Cardiovasc. Pharmacol.* 63:207–212.
16. LeWinter, M. M., and H. L. Granzier. 2013. Titin is a major human disease gene. *Circulation.* 127:938–944.
17. Borlaug, B. A., and W. J. Paulus. 2011. Heart failure with preserved ejection fraction: pathophysiology, diagnosis, and treatment. *Eur. Heart J.* 32:670–679.
18. Yamasaki, R., Y. Wu, …, H. Granzier. 2002. Protein kinase A phosphorylates titin's cardiac-specific N2B domain and reduces passive tension in rat cardiac myocytes. *Circ. Res.* 90:1181–1188.
19. Fukuda, N., Y. Wu, …, H. L. Granzier. 2005. Phosphorylation of titin modulates passive stiffness of cardiac muscle in a titin isoform-dependent manner. *J. Gen. Physiol.* 125:257–271.
20. Krüger, M., S. Kötter, …, W. A. Linke. 2009. Protein kinase G modulates human myocardial passive stiffness by phosphorylation of the titin springs. *Circ. Res.* 104:87–94.
21. Hamdani, N., J. Krysiak, …, W. A. Linke. 2013. Crucial role for Ca2(+)/calmodulin-dependent protein kinase-II in regulating diastolic stress of normal and failing hearts via titin phosphorylation. *Circ. Res.* 112:664–674.
22. Hidalgo, C. G., C. S. Chung, …, H. L. Granzier. 2013. The multifunctional Ca(2+)/calmodulin-dependent protein kinase II delta (CaMKIIδ) phosphorylates cardiac titin's spring elements. *J. Mol. Cell. Cardiol.* 54:90–97.
23. Couchonnal, L. F., and M. E. Anderson. 2008. The role of calmodulin kinase II in myocardial physiology and disease. *Physiology (Bethesda).* 23:151–159.
24. Hagemann, D., M. Kuschel, …, R. P. Xiao. 2000. Frequency-encoding Thr17 phospholamban phosphorylation is independent of Ser16 phosphorylation in cardiac myocytes. *J. Biol. Chem.* 275:22532–22536.
25. Wu, Y., R. J. Colbran, and M. E. Anderson. 2001. Calmodulin kinase is a molecular switch for cardiac excitation-contraction coupling. *Proc. Natl. Acad. Sci. USA.* 98:2877–2881.

26. Dzhura, I., Y. Wu, …, M. E. Anderson. 2002. Cytoskeletal disrupting agents prevent calmodulin kinase, IQ domain and voltage-dependent facilitation of L-type Ca^{2+} channels. *J. Physiol.* 545:399–406.

27. Jaquet, K., K. Fukunaga, …, H. E. Meyer. 1995. A site phosphorylated in bovine cardiac troponin T by cardiac CaM kinase II. *Biochim. Biophys. Acta.* 1248:193–195.

28. Hartzell, H. C., and D. B. Glass. 1984. Phosphorylation of purified cardiac muscle C-protein by purified cAMP-dependent and endogenous Ca^{2+}-calmodulin-dependent protein kinases. *J. Biol. Chem.* 259:15587–15596.

29. Vittone, L., C. Mundina-Weilenmann, and A. Mattiazzi. 2008. Phospholamban phosphorylation by CaMKII under pathophysiological conditions. *Front. Biosci.* 13:5988–6005.

30. Raskin, A., S. Lange, …, F. Sheikh. 2012. A novel mechanism involving four-and-a-half LIM domain protein-1 and extracellular signal-regulated kinase-2 regulates titin phosphorylation and mechanics. *J. Biol. Chem.* 287:29273–29284.

31. Carrion-Vazquez, M., P. E. Marszalek, …, J. M. Fernandez. 1999. Atomic force microscopy captures length phenotypes in single proteins. *Proc. Natl. Acad. Sci. USA.* 96:11288–11292.

32. Nedrud, J., S. Labeit, …, H. Granzier. 2011. Mechanics on myocardium deficient in the N2B region of titin: the cardiac-unique spring element improves efficiency of the cardiac cycle. *Biophys. J.* 101:1385–1392.

33. Leake, M. C., A. Grützner, …, W. A. Linke. 2006. Mechanical properties of cardiac titin's N2B-region by single-molecule atomic force spectroscopy. *J. Struct. Biol.* 155:263–272.

34. Bustamante, C., J. F. Marko, …, S. Smith. 1994. Entropic elasticity of lambda-phage DNA. *Science.* 265:1599–1600.

35. Marko, J. F., and E. D. Siggia. 1994. Fluctuations and supercoiling of DNA. *Science.* 265:506–508.

36. Lee, E. J., J. Peng, …, H. L. Granzier. 2010. Calcium sensitivity and the Frank-Starling mechanism of the heart are increased in titin N2B region-deficient mice. *J. Mol. Cell. Cardiol.* 49:449–458.

37. Chung, C. S., and H. L. Granzier. 2011. Contribution of titin and extracellular matrix to passive pressure and measurement of sarcomere length in the mouse left ventricle. *J. Mol. Cell. Cardiol.* 50:731–739.

38. Kellermayer, M. S., S. B. Smith, …, H. L. Granzier. 1998. Complete unfolding of the titin molecule under external force. *J. Struct. Biol.* 122:197–205.

39. Watanabe, K., P. Nair, …, H. Granzier. 2002. Molecular mechanics of cardiac titin's PEVK and N2B spring elements. *J. Biol. Chem.* 277:11549–11558.

40. Gramlich, M., B. Michely, …, B. Gerull. 2009. Stress-induced dilated cardiomyopathy in a knock-in mouse model mimicking human titin-based disease. *J. Mol. Cell. Cardiol.* 47:352–358.

41. Trombitás, K., A. Freiburg, …, H. Granzier. 1999. Molecular dissection of N2B cardiac titin's extensibility. *Biophys. J.* 77:3189–3196.

42. Trombitás, K., A. Redkar, …, H. Granzier. 2000. Extensibility of isoforms of cardiac titin: variation in contour length of molecular subsegments provides a basis for cellular passive stiffness diversity. *Biophys. J.* 79:3226–3234.

43. Kellermayer, M. S., S. B. Smith, …, H. L. Granzier. 2001. Mechanical fatigue in repetitively stretched single molecules of titin. *Biophys. J.* 80:852–863.

44. Helmes, M., K. Trombitás, …, H. Granzier. 1999. Mechanically driven contour-length adjustment in rat cardiac titin's unique N2B sequence: titin is an adjustable spring. *Circ. Res.* 84:1339–1352.

45. Anderson, B. R., J. Bogomolovas, …, H. Granzier. 2010. The effects of PKCalpha phosphorylation on the extensibility of titin's PEVK element. *J. Struct. Biol.* 170:270–277.

46. Hidalgo, C., B. Hudson, …, H. Granzier. 2009. PKC phosphorylation of titin's PEVK element: a novel and conserved pathway for modulating myocardial stiffness. *Circ. Res.* 105:631–638, 617 p following 638.

47. Mattiazzi, A., R. A. Bassani, …, D. M. Bers. 2015. Chasing cardiac physiology and pathology down the CaMKII cascade. *Am. J. Physiol. Heart Circ. Physiol.* 308:H1177–H1191.

48. Wu, Y., E. D. Luczak, …, M. E. Anderson. 2012. CaMKII effects on inotropic but not lusitropic force frequency responses require phospholamban. *J. Mol. Cell. Cardiol.* 53:429–436.

49. Backs, J., and E. N. Olson. 2006. Control of cardiac growth by histone acetylation/deacetylation. *Circ. Res.* 98:15–24.

50. Anderson, M. E., J. H. Brown, and D. M. Bers. 2011. CaMKII in myocardial hypertrophy and heart failure. *J. Mol. Cell. Cardiol.* 51:468–473.

51. Lorenz, K., J. P. Schmitt, …, M. J. Lohse. 2009. A new type of ERK1/2 autophosphorylation causes cardiac hypertrophy. *Nat. Med.* 15:75–83.

52. Bueno, O. F., and J. D. Molkentin. 2002. Involvement of extracellular signal-regulated kinases 1/2 in cardiac hypertrophy and cell death. *Circ. Res.* 91:776–781.

53. Harris, I. S., S. Zhang, …, A. J. Muslin. 2004. Raf-1 kinase is required for cardiac hypertrophy and cardiomyocyte survival in response to pressure overload. *Circulation.* 110:718–723.

54. Sheikh, F., A. Raskin, …, J. Chen. 2008. An FHL1-containing complex within the cardiomyocyte sarcomere mediates hypertrophic biomechanical stress responses in mice. *J. Clin. Invest.* 118:3870–3880.

55. Lange, S., D. Auerbach, …, E. Ehler. 2002. Subcellular targeting of metabolic enzymes to titin in heart muscle may be mediated by DRAL/FHL-2. *J. Cell Sci.* 115:4925–4936.

56. Hutchinson, K. R., C. Saripalli, …, H. Granzier. 2015. Increased myocardial stiffness due to cardiac titin isoform switching in a mouse model of volume overload limits eccentric remodeling. *J. Mol. Cell. Cardiol.* 79:104–114.

57. Granzier, H. L., K. R. Hutchinson, …, J. E. Smith, 3rd. 2014. Deleting titin's I-band/A-band junction reveals critical roles for titin in biomechanical sensing and cardiac function. *Proc. Natl. Acad. Sci. USA.* 111:14589–14594.

58. Chung, C. S., K. R. Hutchinson, …, H. L. Granzier. 2013. Shortening of the elastic tandem immunoglobulin segment of titin leads to diastolic dysfunction. *Circulation.* 128:19–28.